

# Self-Supervised Learning in Event Sequences: A Comparative Study and Hybrid Approach of Generative Modeling and Contrastive Learning

Viktor Moskvoretskii<sup>1,3,\*</sup>, Dmitry Osin<sup>1,\*</sup>, Egor Shvetsov<sup>1</sup>, Igor Udovichenko<sup>1</sup>, Maxim Zhelnin<sup>1</sup>, Andrey Dukhovny<sup>2</sup>, Anna Zhimerikina<sup>2</sup>, Albert Efimov<sup>2</sup>, Evgeny Burnaev<sup>1</sup>

<sup>1</sup>Skolkovo Institute of Science and Technology

<sup>2</sup>Sberbank

<sup>3</sup>HSE University

{V.Moskvoretskii, d.osin, e.shvetsov, i.udovichenko, M.Zhelnin, e.burnaev}@skoltech.ru,

{Zhimerikina.A.Y, AADukhovny, AREfimov}@sberbank.ru

## Abstract

This study investigates self-supervised learning techniques to obtain representations of Event Sequences (**EvS**). It is a key modality in various applications, including but not limited to banking, e-commerce, and healthcare.

We perform a comprehensive study of generative and contrastive approaches in self-supervised learning, applying them both independently. We find that there is no single supreme method. Consequently, we explore the potential benefits of combining these approaches. To achieve this goal, we introduce a novel method that aligns generative and contrastive embeddings as distinct modalities, drawing inspiration from contemporary multimodal research.

Generative and contrastive approaches are often treated as mutually exclusive, leaving a gap for their combined exploration. Our results demonstrate that this aligned model performs at least on par with, and mostly surpasses, existing methods and is more universal across a variety of tasks. Furthermore, we demonstrate that self-supervised methods consistently outperform the supervised approach on our datasets.

## 1 Introduction

**Motivation.** Event Sequences (**EvS**) are widely used in various real-world applications, including medicine [Waring *et al.*, 2020], biology [Valeri *et al.*, 2023], social media analysis [Liguori *et al.*, 2023], fault diagnosis [Shao *et al.*, 2019], churn prediction [Jain *et al.*, 2021; Sudharsan and Ganesh, 2022], customer segmentation [Carnein and Trautmann, 2019], fraud detection [Xie *et al.*, 2022] and more [Zhuzhel *et al.*, 2023; Fursov *et al.*, 2021]. As a result, there is a growing need to effectively model such data. Most self-supervised methods are focused on images, text, speech, or time-series. In Computer Vision (CV), contrastive learning methods have

achieved state-of-the-art results as a pre-training strategy before supervised fine-tuning [He *et al.*, 2021; Chen *et al.*, 2020; Caron *et al.*, 2021]. In Natural Language Processing (NLP), most modern models rely on generative pre-training [Radford and Narasimhan, 2018; Devlin *et al.*, 2019]. However, these approaches are largely unexplored for **EvS**.

**The aim of our work is** (1) to study generative and contrastive self-supervised approaches for pre-training and representation learning in the domain of **EvS**, (2) and to determine if they can complement each other. We study two ways to combine these approaches. For the first, we use a combined loss function. For the second, drawing inspiration from contemporary multimodal studies [Radford *et al.*, 2021; Zhai *et al.*, 2023; Moskvoretskii and Kuznetsov, 2023] we consider differently pre-trained models as distinct modalities and employ alignment techniques.

**Contributions.** We are the first to our knowledge to examine the generative modeling for pre-training in the domain of **EvS**. We introduce a novel method called the Multimodal-Learning Event Model (MLEM) that aligns two pre-training strategies. Specifically, we use a pre-trained contrastive model to align a generative model. Our results have demonstrated that, on average, the aligned model outperforms any single method across a diverse range of tasks and datasets. Furthermore, our results indicate that self-supervised methods for pre-training outperform supervised approaches on all the datasets we have examined.

Furthermore, our study uncovers two significant insights. First, we find that the generative approach consistently achieves superior performance on tasks related to the Temporal Point Process (TPP), such as predicting the next event type and event time.

Second, we find that most of the methods are robust to perturbations along the time axis. However, they significantly degrade in performance on a synthetic dataset where the time component plays a crucial role. This observation suggests that some event sequences can be sufficiently classified using a "Bag of Words" approach, where the order of events is not as important.

We provide the source code for all the experiments de-

\*These authors contributed equally to this work

scribed in this paper.\*

## 2 Related work

In the following section, we will review various generative, contrastive, hybrid, and other related methods and works.

**Generative methods** for pre-training and representation learning have seen notable development in recent years in both NLP [Radford and Narasimhan, 2018; Devlin *et al.*, 2019; Raffel *et al.*, 2023] and CV [He *et al.*, 2021; Assran *et al.*, 2023; Bachmann *et al.*, 2022]. In NLP one of the generative pre-training procedures is the next token prediction used in BERT [Devlin *et al.*, 2019].

In [Lin *et al.*, 2022] authors study generative modeling of **EvS** for TPP tasks. Similarly to NLP, they use next-event prediction as their main training objective. While **EvS** has been studied in such a generative context, the authors in [Lin *et al.*, 2022] did not specifically investigate generative modeling as a representation of learning or pre-training. The similarities between autoregressive modeling in TPP and the success of generative approaches in NLP have prompted us to consider the potential for applying generative-style self-supervised learning and pre-training to the **EvS** domain.

**Contrastive methods** are a widely recognized in [He *et al.*, 2020; Grill *et al.*, 2020]. These methods typically draw closer the embeddings of variations of the same object and distance them from those of different objects. In CoLES [Babaev *et al.*, 2022] authors study contrastive approach for **EvS**. In their work, the positive samples consist of subsequences derived from a single user’s events, while the negative samples are obtained from events of different users. We utilize this method to examine the efficacy of the contrastive approach in our study.

**Hybrid methods.** Our work falls into the category of hybrid self-supervised approaches [Qi *et al.*, 2023; Yang *et al.*, 2023; Lazarow *et al.*, 2017; Oquab *et al.*, 2023; Zhou *et al.*, 2022; Kim *et al.*, 2021; Kim and Ye, 2022; Shukla and Marlin, 2021]. Few studies have merged generative and contrastive methods, typically focusing on loss combination. DINOv2 [Oquab *et al.*, 2023] updates the traditional contrastive loss from DINO [Caron *et al.*, 2021] with iBOT’s [Zhou *et al.*, 2022] reconstruction loss through Masked Image Modeling. Similarly, GCRL [Kim *et al.*, 2021] combines these losses via a weighted sum, significantly outperforming models that are purely generative or contrastive. EBCLR [Kim and Ye, 2022] also adopts this approach in the context of energy-based models, using a sum of contrastive and generative losses.

Other hybrid methods focus on combining generative and supervised learning [Liu and Abbeel, 2020]. One such method, mTAND [Shukla and Marlin, 2021], has been applied for **EvS** classification.

**Supervised learning** is commonly used for the **EvS** classification task. Some works focus on modeling the underlying

dynamics of the **EvS** process. For example, irregular samples can be modeled by employing dynamic modeling with Ordinary Differential Equations [Rubanova *et al.*, 2019]. In contrast, SeqNAS [Udovichenko *et al.*, 2024] adopts Neural Architecture Search to identify optimal architectures without strong prior assumptions about the underlying process. A key finding is the effectiveness of Recurrent Neural Networks (RNNs) in modeling **EvS**, leading us to incorporate an RNN encoder in our model. Furthermore, the authors propose benchmark datasets for **EvS** classification. We selected the largest datasets from the benchmark, as self-supervised methods require substantial data volumes.

## 3 Event Sequences Preliminaries

Datasets used in this work can be described as sets of sequences:  $C = \{(S_1, y_1), (S_2, y_2), \dots\}$ , where  $y_i$  is an attribute corresponding to the entire sequence or some target. Each  $S_i = ((t_i^1, \Upsilon_i^1), (t_i^2, \Upsilon_i^2), \dots)$  is a sequence of events  $x_i^j = (t_i^j, \Upsilon_i^j)$ , where  $t_i^j$  represents the time when the event  $x_i^j$  occurred and  $t_i^j \leq t_i^{j+1}$ . The set of sub-events  $\Upsilon_i^j = \{k^1, k^2, \dots\}$  describes the event  $x_i^j$ . It is important to note that in this work, the terms *Event Sequences (EvS)* and *Irregularly Sampled Time-series (ISTS)* are used interchangeably, as the occurrence of measurement or sampling for the latter can be seen as an event.

## 4 Methodology

### 4.1 Contrastive Learning

Contrastive Learning encodes a sequence  $S$  into a compact representation  $f_e : S_i \rightarrow h_i \in \mathcal{R}^m$ , by bringing positive pairs (i.e., semantically similar objects) closer to each other in the embedding space, while pushing negative pairs (i.e., dissimilar objects) further apart. In the CoLES [Babaev *et al.*, 2022] framework, the authors suggest constructing a set of positive pairs by sampling sub-sequences from a sequence  $S_i \rightarrow \{S'_i, S''_i\}$ , where each element in  $\{S'_i, S''_i\}$  is shorter than  $S_i$  and elements in  $\{S'_i, S''_i\}$  may intersect, the number of sub-sequences is not limited to two. We adopt this approach and refer to it as the **subsequence sampler** in Figure 1. Further, we utilize loss function (1) from [Hadsell *et al.*, 2006]. The overall procedure is illustrated in Figure 1.

$$L^{con} = \frac{1}{|C|} \sum_{i=1}^{|C|} \sum_{j=1}^{|C|} \left( z_{ij} \frac{1}{2} \|h_i - h_j\|_2^2 + (1 - z_{ij}) \frac{1}{2} \max\{0, \rho - \|h_i - h_j\|_2\}^2 \right) \quad (1)$$

Here,  $z_{ij} \in \{0, 1\}$  denotes if objects are semantically similar,  $h$  is the sequence embedding,  $\rho$  - the minimal margin between dissimilar objects and  $C = \{S_1, S_2, \dots\}$  is a set of sequences.

### 4.2 Generative Modeling

We employ generative modeling to train our bottleneck encoder. Although our methodology is similar to Sequence-to-

\*The source code of our work is publicly available at <https://github.com/VityaVitalich/MLEM>.

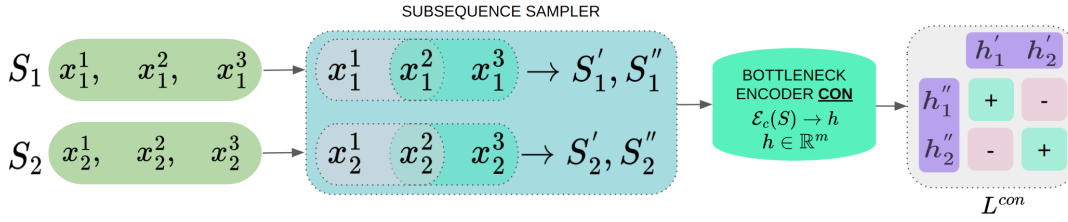


Figure 1: A scheme for contrastive pre-training and representation learning is illustrated using two different sequences,  $\{S_1, S_2\}$ , where  $S \in \mathcal{R}^{l \times f}$  and  $l$  is a sequence and sequence length, respectively. The sub-sequences  $\{S'_1, S'_2, S''_1, S''_2\}$  are sampled using a **subsequence sampler** described in Section 4.1, and the latent representations  $\{h'_1, h'_2, h''_1, h''_2\}$ , where  $h \in \mathbb{R}^m$ , are produced by the contrastive encoder model  $\mathcal{E}_c$ . In our work, we utilize the GRU (Gated Recurrent Unit) and extract the last hidden state as  $h$ . The term  $L^{con}$  denotes the contrastive loss.

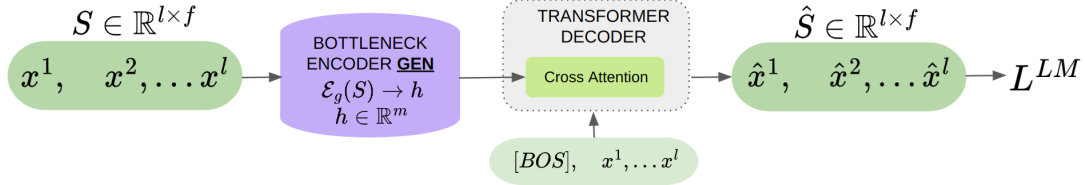


Figure 2: In our generative method, the bottleneck encoder  $\mathcal{E}_g$  encodes the entire sequence  $S \in \mathcal{R}^{l \times f}$  into  $h \in \mathbb{R}^m$ ,  $l$  denotes sequence lengths and  $f$  and  $m$  corresponding hidden sizes. In our work, we utilize the GRU (Gated Recurrent Unit) and extract the last hidden state as  $h$ . For generation, we employ a transformer decoder with recursive generation conditioned on  $h$ . The term  $L^{LM}$  denotes the reconstruction loss, and  $[BOS]$  represents the Beginning Of Sequence token.

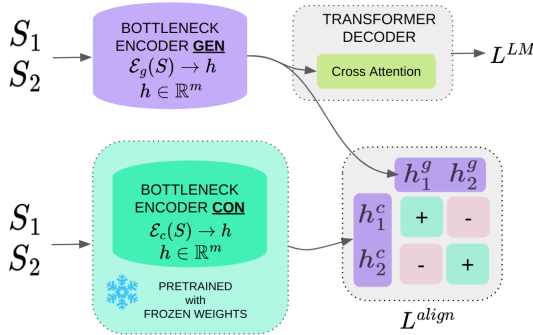


Figure 3: **MLEM** approach for **EvS**. We illustrate it with two different sequences  $\{S_1, S_2\}$ . Both the contrastive **CON** and generative **GEN** encoders map the sequences  $\{S_1, S_2\}$  into corresponding  $\{h_1^c, h_2^c, h_1^g, h_2^g\}$  latent representations. We align the representations from different models using SigLIP and compute the alignment loss,  $L^{align}$  to train **GEN**. Simultaneously we train **GEN** encoder with another reconstruction objective  $L^{LM}$ . In the end, only the **GEN** encoder is used as the final model for fine-tuning and obtaining representations. Throughout the procedure, we use a pre-trained **CON** encoder with frozen weights.

Sequence models, it differs as we use a bottleneck encoder to derive a single vector representation for the entire sequence.

For the encoder, we utilize RNN, which extracts the final hidden state  $h$ , which is subsequently passed into a Transformer decoder [Vaswani *et al.*, 2017]. The decoder reconstructs the entire sequence, conditioned on  $h$  via the Cross-Attention mechanism, in an auto-regressive manner. This entire process is illustrated in Figure 2.

To train the model we use the next event prediction objec-

tive, which is similar to training language models. Nonetheless, as each event in the sequence  $x_i^j = (t_i^j, \Upsilon_i^j)$  contain multiple sub-events  $\Upsilon = \{k^1, k^2, \dots\}$ , we need to reconstruct all of them. To this end, we apply the cross-entropy loss for each categorical  $k$  and the Mean Squared Error (MSE) loss for each real-valued  $k$ . The final loss is a cumulative sum of the losses for all elements in  $\Upsilon = \{k^1, k^2, \dots\}$ , plus the MSE loss for time  $t$ . We denote this loss as  $L^{LM}$ .

Intuitively, this procedure requires our encoder to develop a representation informative enough for the decoder to accurately reconstruct the entire sequence. Since we map all our sequences  $S$  into  $h \in \mathbb{R}^m$  we call all encoders bottleneck encoders.

All details related to the model can be found in Section 5.3.

### 4.3 Aligning generative encoder

To align the embeddings obtained through generative modeling with those acquired through contrastive learning, we treat them as distinct modalities and employ a contrastive aligning procedure inspired by CLIP [Radford *et al.*, 2021]. We utilize the recent SigLIP loss [Zhai *et al.*, 2023] for this purpose. The resulting aligned encoder model is referred to as the Multimodal-Learning Event Model (MLEM).

Overall **MLEM** training procedure is exactly the same as for the generative model described in Section 4.2, except the alignment, which incurs an additional loss (2) resulting in the total loss (3). Training **MLEM** requires a pre-trained contrastive encoder. Using this encoder we train a generative model and align its embeddings with the embeddings produced by the contrastive encoder. Contrastive encoder weights are not updated during training. Both generative

Method	ABank ROC-AUC	Age Accuracy	PhysioNet ROC-AUC	Pendulum MSE	TaoBao ROC-AUC
Supervised	0.768 ± 0.000	0.602 ± 0.005	0.790 ± 0.021	0.33 ± 0.02	0.684 ± 0.002
Contrastive	0.729 ± 0.033	0.638 ± 0.007	<b>0.815 ± 0.013</b>	<b>0.26 ± 0.02</b>	0.679 ± 0.003
Generative	0.788 ± 0.003	0.639 ± 0.007	0.787 ± 0.007	<b>0.26 ± 0.03</b>	<b>0.695 ± 0.004</b>
Naïve	0.658 ± 0.020	0.638 ± 0.007	0.759 ± 0.024	<b>0.26 ± 0.04</b>	0.691 ± 0.002
MLEM	<b>0.790 ± 0.000</b>	<b>0.642 ± 0.005</b>	0.780 ± 0.004	<b>0.26 ± 0.05</b>	<b>0.695 ± 0.002</b>

Table 1: Evaluation of self-supervised methods fine-tuned using supervised loss. ABank, PhysioNet and TaoBao are reported with ROC-AUC, AGE reported with accuracy and Pendulum with MSE.

$\mathcal{E}_g$  and contrastive  $\mathcal{E}_c$  encoders receive a set of sequences  $C = \{S_1, S_2, \dots\}$  and map each sequence  $S$  into corresponding hidden states  $h^g$  and  $h^c$ , then the goal of **MLEM** alignment is to pull embeddings obtained from the same sequence closer to each other and to push embeddings from different sequences further away. This procedure is illustrated in Figure 3. Below is the alignment loss we use:

$$L^{align} = \frac{1}{|C|} \sum_{i=1}^{|C|} \sum_{j=1}^{|C|} \underbrace{\log \frac{1}{1 + e^{z_{ij}(-t \cdot h_i^g \cdot h_j^c + b)}}}_{L_{ij}^{align}} \quad (2)$$

Here,  $z_{ij} \in \{-1, 1\}$  indicates if a pair of embeddings originated from the same sequence  $S$ ,  $t$  and  $b$  denote the temperature and bias, respectively, both are learnable parameters.

Total loss to train **MLEM**:

$$L = \alpha L^{LM}(S, \hat{S}) + \beta L^{align}(\mathcal{E}_g(S), \mathcal{E}_c(S)) \quad (3)$$

Here,  $S$  and  $\hat{S}$  denote original and reconstructed sequences,  $\alpha$  and  $\beta$  are hyperparameters that adjust the strength of alignment.

All technical details can be found in Section 5.3.

#### 4.4 Naïve method

As a baseline, we also examine a straightforward, or Naïve, approach that merges generative and contrastive methods. This is achieved by incorporating a contrastive objective into the generative model, akin to methodologies used in prior studies [Kim *et al.*, 2021; Oquab *et al.*, 2023]. The final loss is a weighted sum of objectives  $L = \alpha L^{LM} + \beta L^{con}$ . One of the downsides of this implementation is that we can not utilize full-length sequences because sub-sequence sampling is required for contrastive procedure. Further, we compare Naïve method with **MLEM** and show that while it is very close by design it leads to inferior results.

## 5 Experiments

### 5.1 Datasets

In our study, we use five **EvS** datasets formally outlined in Section 3.

- A subset of **EvS** datasets from SeqNAS benchmark [Udovichenko *et al.*, 2024], more precisely: ABank, Age, TaoBao. ABank and Age are bank transactions and TaoBao is user activity.

- PhysioNet 2012 comprises highly sparse medical event data, with the goal of predicting mortality.
- Pendulum is a synthetic dataset simulating pendulum motion with the objective of predicting its length using a sequence of coordinates. This dataset was created specifically to evaluate a model’s capability to effectively incorporate the time component in sequence modeling.

Each dataset contains a range of features, both numerical and categorical. All datasets, with the exception of ABank, consist of irregularly sampled time steps. Comprehensive details for each dataset are available in the supplementary materials.

### 5.2 Evaluation objectives

To evaluate the effectiveness of self-supervised training strategies, our study focuses on two key aspects: the quality of the embeddings and the effectiveness of fine-tuning the entire network, following self-supervised studies [Dubois *et al.*, 2024; Dubois *et al.*, 2021].

#### Main Objectives

To assess the quality of embeddings, we primarily rely on metrics from downstream tasks. This involves utilizing both linear and non-linear probing methods. For non-linear probing, we employ Gradient Boosting algorithms with LGBM [Ke *et al.*, 2017] applied directly to the embeddings.

We evaluate embeddings on several tasks, including the prediction of an attribute or a target  $y_i$  given the entire  $S_i$  and the prediction of consequent event  $x^j$  given a set of  $S_i = \{x_i^1, \dots, x_i^{j-1}\}$ . The second objective addresses the TPP task, which involves predicting the type of the next event or the time of the next event’s arrival. We have processed each dataset such that the target is either the category of the next event (for datasets that include this feature) or the time until the next event (for datasets without a primary event category).

#### Secondary Objectives

We incorporate additional metrics to assess the quality of embeddings. Specifically, we utilize anisotropy and intrinsic dimension, drawing on insights from previous research [Nakada and Imaizumi, 2020; Razzhigaev *et al.*, 2023]. In Section 6.3, we compare our findings with the results presented in the aforementioned works.

Anisotropy assesses the non-uniform distribution of embeddings in space, providing insights into the contextualization of our embedding. Lower anisotropy in embeddings

	ABank		Age		PhysioNet		Pendulum		TaoBao	
	ROC-AUC	TPP Acc.	Acc.	TPP Acc.	ROC-AUC	TPP MSE	MSE	TPP MSE	ROC-AUC	TPP Acc.
<b>Linear Probing</b>										
Contrastive	0.678 ± 0.003	0.37	<u>0.623 ± 0.010</u>	0.28	<b>0.819 ± 0.003</b>	<u>1.05</u>	<b>0.37 ± 0.02</b>	<u>0.8</u>	0.680 ± 0.001	0.22
Generative	<u>0.753 ± 0.003</u>	<u>0.43</u>	0.610 ± 0.004	<u>0.3</u>	0.759 ± 0.010	<b>0.93</b>	0.74 ± 0.09	<u>0.8</u>	<b>0.689 ± 0.005</b>	<b>0.35</b>
Naïve	0.703 ± 0.002	0.37	0.602 ± 0.003	<b>0.31</b>	0.733 ± 0.005	<b>0.93</b>	0.59 ± 0.07	<u>0.8</u>	0.680 ± 0.003	0.32
MLEM	<b>0.757 ± 0.000</b>	<b>0.43</b>	<b>0.627 ± 0.000</b>	0.29	<u>0.762 ± 0.010</u>	<b>0.93</b>	<u>0.41 ± 0.01</u>	<b>0.79</b>	<u>0.683 ± 0.003</u>	<b>0.35</b>
<b>Non-linear Probing</b>										
Contrastive	0.691 ± 0.004	0.37	<u>0.629 ± 0.010</u>	0.28	<b>0.822 ± 0.001</b>	<u>1.05</u>	<b>0.37 ± 0.00</b>	<u>0.8</u>	0.686 ± 0.001	0.22
Generative	<u>0.758 ± 0.003</u>	<u>0.43</u>	0.618 ± 0.004	<u>0.3</u>	0.764 ± 0.006	<b>0.93</b>	0.63 ± 0.02	<u>0.8</u>	0.684 ± 0.002	<b>0.35</b>
Naïve	0.704 ± 0.005	0.37	0.608 ± 0.002	<b>0.31</b>	0.774 ± 0.008	<b>0.93</b>	0.57 ± 0.05	<u>0.8</u>	<b>0.690 ± 0.002</b>	0.32
MLEM	<b>0.759 ± 0.003</b>	<b>0.43</b>	<b>0.634 ± 0.005</b>	0.29	<u>0.780 ± 0.001</u>	<b>0.93</b>	<u>0.40 ± 0.01</u>	<b>0.79</b>	<u>0.688 ± 0.002</u>	<b>0.35</b>

Table 2: Evaluation of self-supervised methods using linear and non-linear probing for downstream tasks and TPP tasks. The table reports the mean and standard deviation calculated from three different seeds for downstream task metrics. For TPP tasks, only the mean values from three seeds are presented, as the standard deviation was consistently 0.00. In the table, the best-performing values are highlighted in **bold**, while the second-best values are underlined.

has been linked to better model performance [Ait-Saada and Nadif, 2023]. In line with the approach used in [Razzhigaev *et al.*, 2023], we compute anisotropy as the ratio of the highest singular value to the sum of all singular values:

$$Anisotropy(H) = \frac{\sigma_1^2}{\sum_i \sigma_i^2}$$

The intrinsic dimension evaluates the optimal dimensionality of data, shedding light on the core information captured by the embeddings. To determine the intrinsic dimension, we employ the method proposed in [Facco *et al.*, 2017]. This method examines how the volume of an  $n$ -dimensional sphere changes with dimension  $d$ . Further details are available in the original paper or in [Razzhigaev *et al.*, 2023].

### 5.3 Models

**Feature embeddings.** To transform features into a numerical vector, we use an embedding layer for categorical features and linear projection for numerical ones. For ABank, Age and TaoBao we set the dimension of each feature to 32. For Pendulum and PhysioNet dimension is set to 8. Additionally, we use the time difference between events as a separate feature.

For consistency in our experiments, we use the same encoder architecture across all training strategies and datasets. We use a single-layer GRU with a hidden size of 512, we take the last hidden state as sequence embedding. The GRU is selected for its proven effectiveness in encoding time-ordered sequences and its extensive application in relevant literature, providing a reliable baseline for our study [Rubanova *et al.*, 2019; Tonekaboni *et al.*, 2021; Yoon *et al.*, 2019; Udovichenko *et al.*, 2024].

For **Supervised** model, we use the aforementioned encoder with a linear head.

**Contrastive** learning approach is described at 4.1 and uses the same encoder as mentioned above. Furthermore, we integrate a Feed Forward Projector atop the GRU for loss calculation, a technique commonly adopted in several studies for enhanced performance [Grill *et al.*, 2020; Oquab *et al.*, 2023].

For the **generative** modeling, we employ a vanilla transformer decoder configured with LayerNorm, consisting of 3 layers, 2 heads, a hidden size of 128, and a Feed Forward hidden size of 256. To ensure training stability, we also apply LayerNorm to the sequence embedding produced by the encoder. Additionally, a projection layer is used atop the decoder to predict each feature.

### 5.4 Training details

To maintain consistency in our experiment, we trained all models using identical parameters. Models were trained for 100 epochs on datasets with fewer than 100K sequences and for 40 epochs on larger datasets. The learning rate was set at 1e-3, weight decay at 3e-3, and the batch size was fixed at 128. For the **MLEM** model, we set  $\alpha$  at 1 and  $\beta$  at 10. We averaged the results across three different seeds to ensure reliability and reproducibility.

## 6 Results

### 6.1 Self-supervised pre-training for fine-tuning

Here we evaluate the effectiveness of self-supervised pre-training strategies prior to supervised fine-tuning the entire model. For fine-tuning, we employed pre-trained encoders with randomly initialized linear layers and trained the model for 10 epochs. The results presented in Table 1 indicate that, among all the evaluated pre-training methods, **MLEM** consistently achieves the most favorable results across all datasets, with the exception of the highly sparse PhysioNet dataset. Furthermore, it is noteworthy that supervised learning without self-supervised pre-training consistently produces inferior results.

### 6.2 Embeddings probing

We conducted a comprehensive analysis of the quality of embeddings using both linear and non-linear probing techniques, results are presented in Table 2. We evaluated performance on various tasks described in Section 5.2, including **EvS** classification and regression tasks for the entire sequence, as well as TPP tasks. Despite some variations in absolute values, the overall trends and rankings of methods remain consistent across both probing strategies.

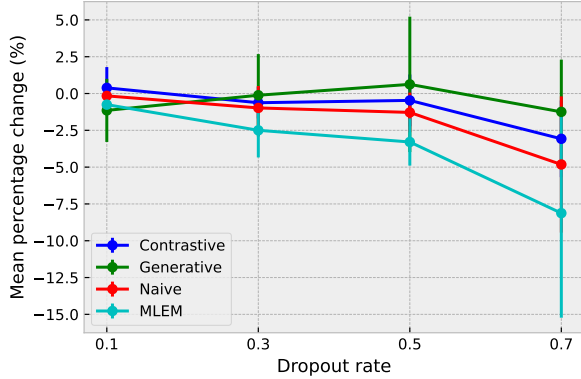


Figure 4: Mean percentage change averaged across datasets. The X-axis represents the dropout probability, while the Y-axis indicates the mean change in the linear probing downstream metric, compared to the metric with no dropout.

Method	Anisotropy ↓	Intrinsic Dimension ↑
Contrastive	$0.11 \pm 0.04$	$10.15 \pm 6.12$
Generative	$0.08 \pm 0.03$	$14.86 \pm 10.12$
Naive	$0.07 \pm 0.04$	$11.26 \pm 6.51$
MLEM	<b><math>0.06 \pm 0.03</math></b>	<b><math>15.86 \pm 9.02</math></b>

Table 3: Average anisotropy and intrinsic dimension across datasets

Our assessment reveals that neither the contrastive nor the generative approach consistently outperforms the other. However, the **MLEM** model consistently demonstrates superior performance across most datasets. Notably, when **MLEM** is not the top performer, it often ranks second, highlighting its versatility. By effectively integrating the advantages of both contrastive and generative techniques, this approach consistently delivers strong overall performance across a range of datasets.

### 6.3 Anisotropy and Intrinsic Dimension

We conducted an evaluation of anisotropy and the intrinsic dimensions of embeddings from various pre-training strategies, as detailed in 5.2. As a result, we show that **MLEM** has the highest intrinsic dimension and the lowest anisotropy, on average, across all datasets. This finding may indicate that our pre-training strategy effectively enables the embeddings to encapsulate a greater amount of information and ensures their uniform distribution in space. The results are presented in Table 3.

Contrary to the findings in [Dubois *et al.*, 2024], we did not observe any correlation between intrinsic dimension and downstream performance metrics. Similarly, we did not find any correlation for anisotropy, which aligns with the aforementioned work.

### 6.4 Visualization

The findings related to anisotropy and intrinsic dimension align with the t-SNE visualization of the Age and TaoBao datasets shown in Figure 6. While contrastive embeddings

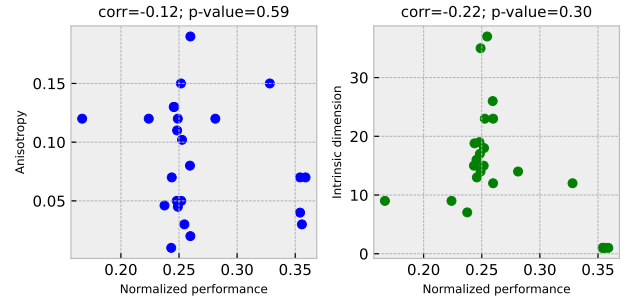


Figure 5: Correlation plots for anisotropy and intrinsic dimension with normalized performance.

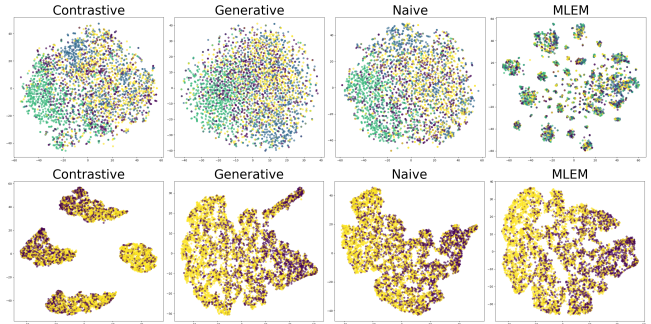


Figure 6: The t-SNE visualizations showcase embeddings resulting from various pre-training strategies. The top row displays the embeddings for the Age dataset, while the bottom row illustrates those for the TaoBao dataset. Each point represents a sequence  $S_i$  from a given dataset, colored accordingly to the corresponding attribute  $y_i$ . For Age, there are 4 classes and 2 classes for TaoBao

typically form distinct clusters, the generative approaches and MLEM provide a more complex embedding space.

## 7 Embedding Robustness

Our study also explores the robustness of model embeddings to specific types of perturbations. We focus on examining the impact of dropout and the shuffling of events within one sequence on the performance of the embeddings on downstream tasks.

### 7.1 Sensitivity to data omission

To investigate the effects of data omission, we applied a random dropout strategy, removing entire events from a sequence along the time axis, with varying probabilities  $p_{dropout} \in \{0.1, 0.3, 0.5, 0.7\}$ . This allowed us to examine the impact of different levels of data removal on the embeddings, as seen in Figure 4, by measuring the average percentage decrease in downstream task metrics.

MLEM’s performance slightly decreases at 0.1 dropout probability and more so at higher levels. This indicates that **MLEM** is more sensitive to dropout and requires the presence of all the samples rather than depending on one specific sample. This property can be used in a sensitivity analysis or related applications.

Additionally, the generative modeling embeddings exhibited an intriguing behavior: they not only resisted the decline but actually surpassed their original performance at a dropout rate of 0.5. To draw reliable conclusions based on this finding, further work is required with a larger number of datasets and various models.

## 7.2 Sensitivity to perturbations

In subsequent tests, we examined the impact of perturbing events within a sequence on downstream task performance. The results, presented in Table 4, show that perturbing sequence elements had minimal to no effect on the results. This suggests that current models may be employing a 'Bag-of-Words' approach and considering a set of events rather than the sequential nature of the data. One might assume that this discrepancy is due to not suitable models or training strategies. However, this hypothesis is not supported by a decline in performance on the pendulum dataset, where the time component is crucial and the same models were used.

This raises the question of whether we could further enhance model performance by explicitly considering the sequential nature of the data, or if this is solely a property of the datasets themselves.

Method	ABank	Age	PhysioNet	Pendulum	TaoBao
Contrastive	+0.47%	-1.93%	-0.37%	-367.57%	-0.15%
Generative	-0.93%	+0.16%	-6.19%	-91.89%	-0.29%
Naive	-1.42%	+0.99%	-3.00%	-147.46%	0.00%
MLEM	-1.45%	-0.16%	-6.56%	-285.37%	+0.29%

Table 4: Percentage change in linear probing performance after shuffling events order

## 8 Computational complexity

To obtain the **MLEM** encoder, we need to train two models, which is not desirable. However, to demonstrate the practicality of our method, we compare **MLEM** with SeqNas [Udovichenko *et al.*, 2024] in terms of performance and computational efficiency. SeqNas employs an architectural search to identify the most optimal supervised architecture for the task at hand. We posit that SeqNas represents an upper bound for downstream metrics. Table 5 presents results from the two largest datasets, examined by us, demonstrating that **MLEM** achieves performance near the upper bound set by SeqNas, but with significantly lower computational cost.

Method	ABank		Age	
	ROC-AUC	GPU hours	Accuracy	GPU hours
MLEM	0.790 ± 0.000	25	0.642 ± 0.005	9
SeqNas	0.7963 ± 0.001	288	0.645 ± 0.002	80

Table 5: Comparison of downstream metrics and computational costs for training and fine-tuning **MLEM** versus **SeqNas**.

## 9 Discussion

We observe that in our settings, **MLEM** outperforms the Naïve method, despite their initial similarities. One possible

explanation for the success of our method can be attributed to viewing **MLEM** as a Knowledge Distillation [Hinton *et al.*, 2015] procedure. However, further work is required to confirm this hypothesis.

We observed that data perturbation does not significantly impact model performance, suggesting a near-time-invariance. This could be attributed to the nature of the examined datasets or the absence of appropriate modeling approaches. Both hypotheses suggest the potential for future research in time-sensitive modeling.

We also observe consistent underperformance of methods that include generative approach on the PhysioNet dataset. This could be attributed to the high rate of missing values, which complicates the generation of accurate predictions for subsequent steps. Furthermore, the relatively small size of the dataset may be a contributing factor, given that generative modeling is generally dependent on large amounts of data.

## 10 Conclusion

We proposed a novel approach to combine multiple self-supervised strategies and demonstrated that this approach yields superior results compared to any single self-supervised method. We believe this opens up a new direction for enhancing self-supervised learning.

Our study revealed that self-supervised pre-trained models, especially those with generative pre-training, outperform purely supervised methods, with **MLEM** showing the most promise. This suggests potential benefits in exploring different pre-training and architectural options.

In our work, we are the first, to our knowledge, to apply generative modeling to event sequences for representation learning and pre-training. Our findings show that neither generative nor contrastive pre-training clearly surpasses the other in effectiveness. To address this, we developed the **MLEM** method, which innovatively merges contrastive learning with generative modeling. **MLEM** aligns these two approaches as separate modalities, inspired by recent advances in multimodal research, and it demonstrates enhanced performance on most datasets for both primary and secondary goals.

## References

- [Ait-Saada and Nadif, 2023] Mira Ait-Saada and Mohamed Nadif. Is anisotropy truly harmful? a case study on text clustering. In Anna Rogers, Jordan Boyd-Graber, and Naoaki Okazaki, editors, *Proceedings of the 61st Annual Meeting of the Association for Computational Linguistics (Volume 2: Short Papers)*, pages 1194–1203, Toronto, Canada, July 2023. Association for Computational Linguistics.
- [Assran *et al.*, 2023] Mahmoud Assran, Quentin Duval, Ishan Misra, Piotr Bojanowski, Pascal Vincent, Michael Rabbat, Yann LeCun, and Nicolas Ballas. Self-supervised learning from images with a joint-embedding predictive architecture, 2023.
- [Babaev *et al.*, 2022] Dmitrii Babaev, Nikita Ovsov, Ivan Kireev, Maria Ivanova, Gleb Gusev, Ivan Nazarov, and Alexander Tuzhilin. Coles: contrastive learning for event sequences with self-supervision. In *Proceedings of the 2022 International Conference on Management of Data*, pages 1190–1199, 2022.
- [Bachmann *et al.*, 2022] Roman Bachmann, David Mizrahi, Andrei Atanov, and Amir Zamir. Multimaes: Multi-modal multi-task masked autoencoders, 2022.
- [Carnein and Trautmann, 2019] Matthias Carnein and Heike Trautmann. Customer segmentation based on transactional data using stream clustering. In *Advances in Knowledge Discovery and Data Mining: 23rd Pacific-Asia Conference, PAKDD 2019, Macau, China, April 14-17, 2019, Proceedings, Part I 23*, pages 280–292. Springer, 2019.
- [Caron *et al.*, 2021] Mathilde Caron, Hugo Touvron, Ishan Misra, Hervé Jégou, Julien Mairal, Piotr Bojanowski, and Armand Joulin. Emerging properties in self-supervised vision transformers, 2021.
- [Chen *et al.*, 2020] Ting Chen, Simon Kornblith, Mohammad Norouzi, and Geoffrey Hinton. A simple framework for contrastive learning of visual representations, 2020.
- [Devlin *et al.*, 2019] Jacob Devlin, Ming-Wei Chang, Kenton Lee, and Kristina Toutanova. Bert: Pre-training of deep bidirectional transformers for language understanding, 2019.
- [Dubois *et al.*, 2021] Yann Dubois, Douwe Kiela, David J. Schwab, and Ramakrishna Vedantam. Learning optimal representations with the decodable information bottleneck, 2021.
- [Dubois *et al.*, 2024] Yann Dubois, Tatsunori Hashimoto, and Percy Liang. Evaluating self-supervised learning via risk decomposition, 2024.
- [Facco *et al.*, 2017] Elena Facco, Maria d’Errico, Alex Rodriguez, and Alessandro Laio. Estimating the intrinsic dimension of datasets by a minimal neighborhood information. *Scientific Reports*, 7(1), September 2017.
- [Fursov *et al.*, 2021] Ivan Fursov, Matvey Morozov, Nina Kaploukhaya, Elizaveta Kovtun, Rodrigo Rivera-Castro, Gleb Gusev, Dmitriy Babaev, Ivan Kireev, Alexey Zaytsev, and Evgeny Burnaev. Adversarial attacks on deep models for financial transaction records, 2021.
- [Grill *et al.*, 2020] Jean-Bastien Grill, Florian Strub, Florent Alché, Corentin Tallec, Pierre H. Richemond, Elena Buchatskaya, Carl Doersch, Bernardo Avila Pires, Zhao-han Daniel Guo, Mohammad Gheshlaghi Azar, Bilal Piot, Koray Kavukcuoglu, Rémi Munos, and Michal Valko. Bootstrap your own latent: A new approach to self-supervised learning, 2020.
- [Hadsell *et al.*, 2006] Raia Hadsell, Sumit Chopra, and Yann Lecun. Dimensionality reduction by learning an invariant mapping. pages 1735 – 1742, 02 2006.
- [He *et al.*, 2020] Kaiming He, Haoqi Fan, Yuxin Wu, Saining Xie, and Ross Girshick. Momentum contrast for unsupervised visual representation learning, 2020.
- [He *et al.*, 2021] Kaiming He, Xinlei Chen, Saining Xie, Yanghao Li, Piotr Dollár, and Ross Girshick. Masked autoencoders are scalable vision learners, 2021.
- [Hinton *et al.*, 2015] Geoffrey Hinton, Oriol Vinyals, and Jeff Dean. Distilling the knowledge in a neural network. *arXiv preprint arXiv:1503.02531*, 2015.
- [Jain *et al.*, 2021] Hemlata Jain, Ajay Khunteta, and Sumit Srivastava. Telecom churn prediction and used techniques, datasets and performance measures: a review. *Telecommunication Systems*, 76:613–630, 2021.
- [Ke *et al.*, 2017] Guolin Ke, Qi Meng, Thomas Finley, Taifeng Wang, Wei Chen, Weidong Ma, Qiwei Ye, and Tie-Yan Liu. Lightgbm: A highly efficient gradient boosting decision tree. In I. Guyon, U. Von Luxburg, S. Bengio, H. Wallach, R. Fergus, S. Vishwanathan, and R. Garnett, editors, *Advances in Neural Information Processing Systems*, volume 30. Curran Associates, Inc., 2017.
- [Kim and Ye, 2022] Beomsu Kim and Jong Chul Ye. Energy-based contrastive learning of visual representations, 2022.
- [Kim *et al.*, 2021] Saehoon Kim, Sungwoong Kim, and Juho Lee. Hybrid generative-contrastive representation learning, 2021.
- [Lazarow *et al.*, 2017] Justin Lazarow, Long Jin, and Zhuowen Tu. Introspective neural networks for generative modeling. In *Proceedings of the IEEE International Conference on Computer Vision*, pages 2774–2783, 2017.
- [Liguori *et al.*, 2023] Angelica Liguori, Luciano Caroprese, Marco Minici, Bruno Veloso, Francesco Spinnato, Mirco Nanni, Giuseppe Manco, and Joao Gama. Modeling events and interactions through temporal processes—a survey. *arXiv preprint arXiv:2303.06067*, 2023.
- [Lin *et al.*, 2022] Haitao Lin, Lirong Wu, Guojiang Zhao, Pai Liu, and Stan Z Li. Exploring generative neural temporal point process. *arXiv preprint arXiv:2208.01874*, 2022.
- [Liu and Abbeel, 2020] Hao Liu and Pieter Abbeel. Hybrid discriminative-generative training via contrastive learning. *arXiv preprint arXiv:2007.09070*, 2020.

- [Moskvoretskii and Kuznetsov, 2023] Viktor Moskvoretskii and Denis Kuznetsov. Imad: Image-augmented multi-modal dialogue. *arXiv preprint arXiv:2305.10512*, 2023.
- [Nakada and Imaizumi, 2020] Ryumei Nakada and Masaaki Imaizumi. Adaptive approximation and generalization of deep neural network with intrinsic dimensionality, 2020.
- [Oquab *et al.*, 2023] Maxime Oquab, Timothée Darcet, Théo Moutakanni, Huy Vo, Marc Szafraniec, Vasil Khilidov, Pierre Fernandez, Daniel Haziza, Francisco Massa, Alaaeldin El-Nouby, Mahmoud Assran, Nicolas Ballas, Wojciech Galuba, Russell Howes, Po-Yao Huang, Shang-Wen Li, Ishan Misra, Michael Rabbat, Vasu Sharma, Gabriel Synnaeve, Hu Xu, Hervé Jegou, Julien Mairal, Patrick Labatut, Armand Joulin, and Piotr Bojanowski. DINOv2: Learning robust visual features without supervision, 2023.
- [Qi *et al.*, 2023] Zekun Qi, Runpei Dong, Guofan Fan, Zheng Ge, Xiangyu Zhang, Kaisheng Ma, and Li Yi. Contrast with reconstruct: Contrastive 3d representation learning guided by generative pretraining. *arXiv preprint arXiv:2302.02318*, 2023.
- [Radford and Narasimhan, 2018] Alec Radford and Karthik Narasimhan. Improving language understanding by generative pre-training, 2018.
- [Radford *et al.*, 2021] Alec Radford, Jong Wook Kim, Chris Hallacy, Aditya Ramesh, Gabriel Goh, Sandhini Agarwal, Girish Sastry, Amanda Askell, Pamela Mishkin, Jack Clark, Gretchen Krueger, and Ilya Sutskever. Learning transferable visual models from natural language supervision, 2021.
- [Raffel *et al.*, 2023] Colin Raffel, Noam Shazeer, Adam Roberts, Katherine Lee, Sharan Narang, Michael Matena, Yanqi Zhou, Wei Li, and Peter J. Liu. Exploring the limits of transfer learning with a unified text-to-text transformer, 2023.
- [Razhigaev *et al.*, 2023] Anton Razhigaev, Matvey Mikhalechuk, Elizaveta Goncharova, Ivan Oseledets, Denis Dimitrov, and Andrey Kuznetsov. The shape of learning: Anisotropy and intrinsic dimensions in transformer-based models, 2023.
- [Rubanova *et al.*, 2019] Yulia Rubanova, Ricky T. Q. Chen, and David Duvenaud. Latent odes for irregularly-sampled time series, 2019.
- [Shao *et al.*, 2019] Siyu Shao, Ruqiang Yan, Yadong Lu, Peng Wang, and Robert X Gao. Dcn-based multi-signal induction motor fault diagnosis. *IEEE Transactions on Instrumentation and Measurement*, 69(6):2658–2669, 2019.
- [Shukla and Marlin, 2021] Satya Narayan Shukla and Benjamin M. Marlin. Multi-time attention networks for irregularly sampled time series, 2021.
- [Sudharsan and Ganesh, 2022] R Sudharsan and EN Ganesh. A swish rnn based customer churn prediction for the telecom industry with a novel feature selection strategy. *Connection Science*, 34(1):1855–1876, 2022.
- [Tonekaboni *et al.*, 2021] Sana Tonekaboni, Danny Eytan, and Anna Goldenberg. Unsupervised representation learning for time series with temporal neighborhood coding, 2021.
- [Udovichenko *et al.*, 2024] Igor Udovichenko, Egor Shvetsov, Denis Divitsky, Dmitry Osin, Ilya Trofimov, Ivan Sukharev, Anatoliy Glushenko, Dmitry Berestnev, and Evgeny Burnaev. SeqNAS: Neural architecture search for event sequence classification. *IEEE Access*, 12:3898–3909, 2024.
- [Valeri *et al.*, 2023] Jacqueline A Valeri, Luis R Soenksen, Katherine M Collins, Pradeep Ramesh, George Cai, Rani Powers, Nicolaas M Angenent-Mari, Diogo M Camacho, Felix Wong, Timothy K Lu, et al. Bioautomated: An end-to-end automated machine learning tool for explanation and design of biological sequences. *Cell Systems*, 14(6):525–542, 2023.
- [Vaswani *et al.*, 2017] Ashish Vaswani, Noam Shazeer, Niki Parmar, Jakob Uszkoreit, Llion Jones, Aidan N Gomez, Łukasz Kaiser, and Illia Polosukhin. Attention is all you need. *Advances in neural information processing systems*, 30, 2017.
- [Waring *et al.*, 2020] Jonathan Waring, Charlotta Lindvall, and Renato Umerton. Automated machine learning: Review of the state-of-the-art and opportunities for healthcare. *Artificial intelligence in medicine*, 104:101822, 2020.
- [Xie *et al.*, 2022] Yu Xie, GuanJun Liu, Chungang Yan, ChangJun Jiang, and MengChu Zhou. Time-aware attention-based gated network for credit card fraud detection by extracting transactional behaviors. *IEEE Transactions on Computational Social Systems*, 2022.
- [Yang *et al.*, 2023] Yonghui Yang, Zhengwei Wu, Le Wu, Kun Zhang, Richang Hong, Zhiqiang Zhang, Jun Zhou, and Meng Wang. Generative-contrastive graph learning for recommendation. 2023.
- [Yoon *et al.*, 2019] Jinsung Yoon, Daniel Jarrett, and Mihaela van der Schaar. Time-series generative adversarial networks. In H. Wallach, H. Larochelle, A. Beygelzimer, F. d'Alché-Buc, E. Fox, and R. Garnett, editors, *Advances in Neural Information Processing Systems*, volume 32. Curran Associates, Inc., 2019.
- [Zhai *et al.*, 2023] Xiaohua Zhai, Basil Mustafa, Alexander Kolesnikov, and Lucas Beyer. Sigmoid loss for language image pre-training, 2023.
- [Zhou *et al.*, 2022] Jinghao Zhou, Chen Wei, Huiyu Wang, Wei Shen, Cihang Xie, Alan Yuille, and Tao Kong. ibot: Image bert pre-training with online tokenizer, 2022.
- [Zhuzhel *et al.*, 2023] Vladislav Zhuzhel, Vsevolod Grabar, Galina Boeva, Artem Zabolotnyi, Alexander Stepikin, Vladimir Zholobov, Maria Ivanova, Mikhail Orlov, Ivan Kireev, Evgeny Burnaev, et al. Continuous-time convolutions model of event sequences. *arXiv preprint arXiv:2302.06247*, 2023.

## Detailed Dataset Information

Detailed information regarding all the datasets is presented in Table 6.

**ABank** is a dataset of bank transactions with regularly sampled time-steps, representing transaction IDs rather than the transaction times. The goal is binary classification: predicting whether a user will default.

**Age** consists of bank transactions with irregularly sampled time-steps. The task is to categorize users into one of four age groups.

**PhysioNet** features medical measurements with irregularly sampled time-steps. The target is binary classification: predicting in-hospital mortality.

**Pendulum** is a synthetic dataset created from pendulum simulations with irregularly sampled time-steps, using the Hawkes process. It includes features like the x and y coordinates of the pendulum, normalized by its length. Each observation has a unique real-valued pendulum length, and the task is to predict this length. The detailed dataset synthesis procedure is described in section Pendulum dataset generation.

**Taobao** captures user activity on the TaoBao platform with irregular time-steps. The binary classification task is to predict whether a user will make a payment in the next 7 days.

For all datasets, categories that appeared fewer than 500 times were consolidated into a single category. Event time values were normalized to a unit interval for consistency. In the case of the PhysioNet dataset, features were aggregated at 360-second intervals. If a feature appeared at least once within this timeframe, its average was calculated. If a feature was absent, it was marked with a value of -1. No other manual feature generation or specific preprocessing was performed, unless otherwise specified.

**Train - test - validation splits.** For test sets we followed existing literature [Babaev *et al.*, 2022; Udovichenko *et al.*, 2024], with the exception of the PhysioNet dataset, for which we created the split. The train and validation sets for each training session were random in fixed proportions. All the metrics are reported on test sets. In cases where sequences exceeded a specified length, we selected the  $N$  most recent events, with  $N$  being the sequence length as defined in dataset Table 6.

## Pendulum dataset generation

We developed a pendulum dataset to assess models when time dependency is crucial.

We simulated pendulum motion with different lengths and sampled coordinates with irregular time intervals, which were derived using a sampling method based on the Hawkes process. Therefore, our dataset consists of sequences where each event is represented with time and two coordinates, each sequence is generated with different pendulum length.

We opted to Hawkes process to emphasize the critical role of accurate event timing in successful model performance corresponding to real world applications.



Figure 7: The figure illustrates the pendulum motion at various instances, with time steps determined by a Hawkes process. It captures the pendulum’s trajectory using only the normalized planar coordinates at these sampled times.



Figure 8: Example of temporal distribution of events ranging from 0 to 5 seconds. Each event is marked with a star along the timeline. The y-axis serves only as a technical aid to separate the events for clarity and does not convey any additional information.

To model the Hawkes process, we consider the following intensity function  $\lambda(t)$  that is given by (4).

$$\lambda(t) = \mu + \sum_{t_i < t} \alpha e^{-\beta(t-t_i)} \quad (4)$$

We used following parameters for the Hawkes process:

- $\mu$  is the base intensity, was fixed at 10;
- $\alpha$  is the excitation factor, was chosen to be 0.2;
- $\beta$  is the decay factor, was set to 1.
- $t_i$  are the times of previous events before time  $t$ .

The example of generated event times with these parameters is depicted in Figure 8.

These parameter values were selected with the intention of generating sequences that contained approximately 100 events each. Additionally, this specific combination of  $\mu$ ,  $\alpha$ , and  $\beta$  was designed to create sequences where events would be densely clustered during certain intervals and sparsely distributed during others. This configuration allowed us to simulate scenarios that closely mimic real-world dynamics, where event occurrences can fluctuate between periods of high and low activity.

To model the pendulum we consider the second-order differential equation:

$$\theta'' + \left(\frac{b}{m}\right) \theta' + \left(\frac{g}{L}\right) \sin(\theta) = 0 \quad (5)$$

where,

- $\theta''$  is the Angular Acceleration,
- $\theta'$  is the Angular Velocity,
- $\theta$  is the Angular Displacement,
- $b$  is the Damping Factor,
- $g = 9.81 \text{ m/s}^2$  is the acceleration due to gravity,
- $L$  is the Length of pendulum,

	ABank	Age	Taobao	PhysioNet	Pendulum
# Observations	2.7B	26B	7.8M	0.5M	8.9M
Mean observations per user	280	881	806	72	89
Observations std. per user	270	124	1042	21	11
Max observations per user in modeling	200	1000	1000	200	200
# Sequences	963M	30K	9K	8K	100K
# Classes	2	4	2	2	-
# Categorical features	16	1	2	3	0
# Real-valued features	3	1	0	38	2
Target	Default	Age group	Payment	Mortality	Length

Table 6: Statistics of datasets

- $m$  is the Mass of bob in kg.

To convert this second-order differential equation into two first-order differential equations, we let  $\theta_1 = \theta$  and  $\theta_2 = \theta'$ , which gives us:

$$\theta_2' = \theta_2'' = -\left(\frac{b}{m}\right)\theta_2 - \left(\frac{g}{L}\right)\sin(\theta_1) \quad (6)$$

$$\theta_1' = \theta_2 \quad (7)$$

Thus, the first-order differential equations for the pendulum simulation are:

$$\theta_2' = -\left(\frac{b}{m}\right)\theta_2 - \left(\frac{g}{L}\right)\sin(\theta_1) \quad (8)$$

$$\theta_1' = \theta_2 \quad (9)$$

In our simulations, we fixed the damping factor  $b = 0.5$  and the mass of the bob  $m = 1$ . The length  $L$  of the pendulum is taken from a uniform distribution  $U(0.5, 5)$ , representing a range of possible lengths from 0.5 to 5 meters. The initial angular displacement  $\theta$  and the initial angular velocity  $\theta'$  are both taken from a uniform distribution  $U(1, 9)$ , which provides a range of initial conditions in radians and radians per second, respectively.

Our primary objective is to predict the length of the pendulum, denoted as  $L$ , using the normalized coordinates  $x$  and  $y$  on the plane. These coordinates are scaled with respect to the pendulum’s length, such that the trajectory of the pendulum is represented in a unitless fashion. This normalization allows us to abstract the pendulum’s motion from its actual physical dimensions and instead focus on the pattern of movement. An illustrative example of this motion is presented in Figure 7, where the path traced by the pendulum bob is depicted over time.

## Generated datasets

We conducted a preliminary evaluation of our decoder’s ability to reconstruct sequences from their embeddings. We hypothesize that while the regenerated sequences may exhibit slight deviations from the original data, the overall distribution of features across whole dataset should align. To investigate this, we compared distributions of features in generated datasets, results are visualized in Figure 9 for Age dataset.

There is a notable resemblance between the generated sequences and the actual data regarding the distribution of

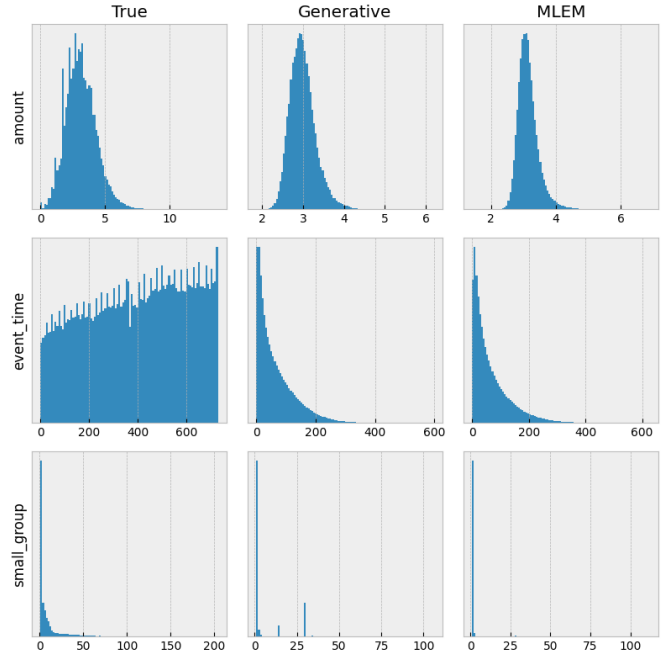


Figure 9: Distributions of features for real and generated Age dataset. True denotes distributions for real dataset, Generative and MLEM denote distributions for datasets generated from embeddings obtain via Generative and MLEM approaches.

numerical feature ”amount”, particularly around the mean. However, the model struggles with accurately reproducing the timing and the key dataset feature—the user group. The MLEM tends to overrepresent the most frequent classes while underrepresenting less common ones. Moreover, the Generative model despite of the mostly same performance exhibits unexpected behaviour, overproducing some of the rarer classes.

These findings suggest directions for potential improvements, more specifically: improving time component modeling, applying different generation approaches, and studying different architecture designs such as enhancing either the encoder’s or decoder’s performance.